ISSUES IN PRODUCTION OF CARBON NANOTUBES AND RELATED NANOCOMPOSITES: A COMPREHENSIVE REVIEW

M. HASANZADEH,[*] V. MOTTAGHITALAB,[*] R. ANSARI,[**]
B. HADAVI MOGHADAM[*] and A. K. HAGHI[*]

[*]*Department of Textile Engineering, University of Guilan, Rasht, Iran*
[**]*Department of Mechanical Engineering, University of Guilan, Rasht, Iran*
✉ *Corresponding author: A. K. Haghi, AKHaghi@yahoo.com*

Received July 10, 2013

Polymer nanofibers are being increasingly used for a wide range of applications owing to their high specific surface area. The electrospinning process, as a novel and effective method for producing nanofibers from various materials, has been utilized to fabricate nanofibrous membranes. Carbon nanotubes (CNTs) have a number of outstanding mechanical, electrical, and thermal properties, which make them attractive as reinforcement in a polymer matrix. The incorporation of CNT into polymer nanofibers can improve the properties of electrospun nanofibrous composites. This paper provides a comprehensive review of current research and development in the field of electrospun CNT-polymer composite nanofiber with emphasis on the processing, properties, and application of composite nanofiber, as well as the theoretical approaches to predicting the mechanical behavior of CNT-polymer composites. The current limitations, research challenges, and future trends in modeling and simulation of electrospun polymer composite nanofibers are also discussed.

Keywords: carbon nanotube, electrospinning, mechanical properties, theoretical approaches

INTRODUCTION

With the rapid development and growing role of nanoscience and nanotechnology in recent years, considerable research efforts have been directed towards the development and characterization of fibrous materials with a diameter in the range of tens to hundreds of nanometers.[1-4]

Electrospinning, as a simple and powerful technique for producing ultrafine fibers, has evinced more interest and attention in recent years.[5-10] In this process, the nanofibers are generated by the application of a strong electric field on a polymer solution or melt. The sub-micron-range spun fibers produced by this technique possess high specific surface area, high porosity, and small pore size.[11-15] Electrospun polymer nanofibers are very attractive multifunctional nanostructures due to their versatility and potential for diverse applications. Some of these notable applications include tissue engineering scaffolds,[16-18] biomedical agents,[19] protective clothing,[20] drug delivery,[21] super capacitors,[22,23] and energy storage.[24]

Carbon nanotubes (CNTs) are highly desirable materials possessing unique structural, mechanical, thermal, and electrical properties.[25-30] Electrospun nanotube-polymer composite nanofibers are very attractive materials for a wide range of applications. This is due to the fact that the use of the electrospinning technique to incorporate CNTs in polymer nanofibers induces the alignment of nanotubes within the nanofiber structure, which could greatly enhance the mechanical, electrical and thermal properties of composite fibers.[31-34]

Numerous studies have focused on understanding and improving the structure and properties of electrospun CNT-polymer composites.[35-45] However, due to the difficulties encountered in the experimental characterization of nanomaterials, the simulation and theoretical approaches play a significant role in understan-

ding the properties and mechanical behavior of CNT-reinforced polymer nanofibers.[46]

The current review summarizes the recent progress made in electrospun CNT-polymer composite nanofibers, along with their processing, characterization, mechanical properties, and applications. Theoretical investigations on mechanical properties of CNT and CNT-based polymer composites are also addressed. Finally, research challenges and future trends in modeling and simulation of electrospun polymer composite nanofibers are discussed.

FUNDAMENTALS OF ELECTROSPINNING

Concepts and mechanism

Electrospinning, as a straightforward, simple and effective method for the preparation of nanofibrous materials, has attracted increasing attention during the last two decades.[5-10] The electrospinning process, unlike the conventional fiber spinning systems (melt spinning, wet spinning, etc.), uses electric field force instead of mechanical force to draw and stretch a polymer jet.[47] This process involves three main components, including a syringe filled with a polymer solution, a high voltage supplier to provide the required electric force for stretching the liquid jet, and a grounded collection plate to hold the nanofiber mat. A schematic representation of the electrospinning setup is shown in Figure 1. In the electrospinning process, when the electric field overcomes the surface tension force of the droplet of the polymer solution formed on the tip of the syringe, the charged polymer solution forms a liquid jet and travels towards the collection plate. The ejected polymer solution forms a conical shape known as the "Taylor cone" and is drawn towards a grounded collection plate.[48-60]

The electrospinning process can be explained by four major regions, including the Taylor cone region, the stable jet region, the instability region, and the base region. Once the electric field reaches a critical value, a charged jet of the solution is ejected from the tip of the Taylor cone and will begin to thin due to the forces acting on it. The thinning of the jet can be divided into two different stages. The initial stage is a period of thinning as a straight jet and the later stage is a period of thinning due to the bending/whipping instability. Typically, the electrospinning process has four types of physical instability: the classical Rayleigh instability, the axisymmetric instability, the bending instability, which results in whipping, and the whipping instability. These instabilities influence the morphology and the structure of the deposited fibers.[61-65] Figure 2 illustrates the four types of instability of the jet.

Rayleigh instability is axisymmetric and is commonly observed in low electric field strength (low charge densities) or when the viscosity of the solution is below the optimum value. This instability causes the liquid jet to break up due to the surface tension force. At high electric fields, the Rayleigh instability disappears and is replaced by a bending instability. Both the bending and whipping (non-axisymmetric) instabilities occur owing to the charge-charge repulsion between the excess charges present in the jet.

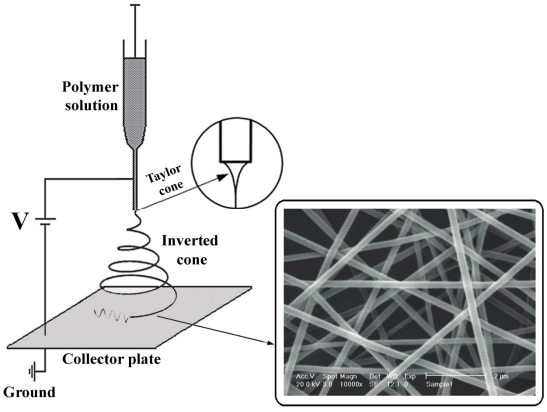

Figure 1: Schematic drawing of the electrospinning process

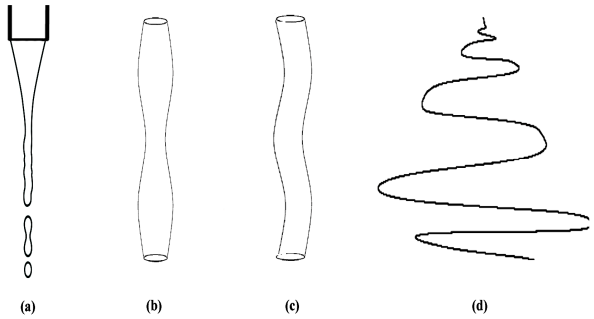

Figure 2: Instabilities in the jet (a) Rayleigh instability, (b) axisymmetric conducting instability, (c) bending instability and (d) whipping instability

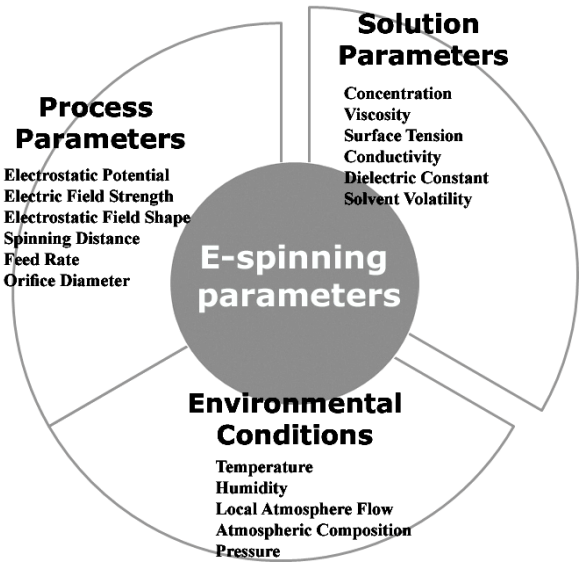

Figure 3: Electrospinning parameters known to affect the resultant nanofiber morphology

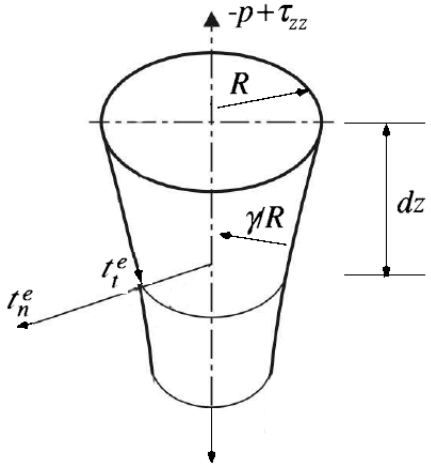

Figure 4: Momentum balance on a short section of the jet; adapted from Feng [62]

The bending instability produces oscillations in the diameter of the jet in the axial direction caused by electrical forces (see Figure 2).The non-axisymmetric instability replaces the axisymmetric (i.e., Rayleigh and bending) instabilities at higher electric fields and produces a bending and stretching force on the jet.[61]

The morphology and the structure of the electrospun nanofibers are dependent upon many parameters, which are mainly divided into three categories: solution properties, processing parameters, and ambient conditions, as illustrated in Figure 3.[66-68]

Governing equations

The analysis of the electrospinning process is based on the slender-body theory. It is widely used in fiber spinning of viscoelastic liquid. To simplify the mathematical description, a few idealizing assumptions are made. The jet radius R decreases slowly along the axial direction $Z:\left|dR(Z)/dZ\right| \ll 1$. Furthermore, it is assumed that the fluid velocity v is uniform in the cross section of the jet.

The basic governing equations for the stable jet region are the equation of continuity, conservation of electric charges, linear

momentum balance, and electric field equation. As main sources for these flow equations, we refer to Haghi *et al.*; Feng; Carroll *et al.*[1,62,69]

The most important and the simplest relation is the equation of continuity; it describes the conservation of mass in electrospinning:

$$\pi R^2 \upsilon = Q \tag{1}$$

where Q is a constant volume flow rate. The conservation of electric charge may be expressed by:

$$\pi R^2 KE + 2\pi R \upsilon \sigma = I \tag{2}$$

where K is the electrical conductivity of the liquid jet, E is the axial component of the electric field, σ is the surface charge density, and I is the constant total current in the jet. The conservation of momentum for the fluid is formulated by the relation: (see Figure 4)

$$\frac{d}{dz}(\pi R^2 \rho \upsilon^2) = \pi R^2 \rho g + \frac{d}{dz}[\pi R^2(-p + \tau_{zz})] + \frac{\gamma}{R}.2\pi R R' + 2\pi R(t_t^e - t_n^e R')$$

where ρ is the fluid density, g is the acceleration due to gravity, p is the pressure, τ_{ZZ} is the axial viscous normal stress, γ is the surface tension, and t_t^e and t_n^e are the tangential and normal tractions, respectively, on the surface of the jet due to electricity. The prime indicates a derivative with respect to z, and R' is the slope of the jet surface. The ambient pressure has been set to zero. The electrostatic tractions are determined by the surface charge density and the electric field:

$$t_n^e = \left\| \frac{\varepsilon}{2}(E_n^2 - E_t^2) \right\| \approx \frac{\sigma^2}{2\bar{\varepsilon}} - \frac{\bar{\varepsilon} - \varepsilon}{2} E^2 \tag{4}$$

$$t_t^e = \sigma E_t \approx \sigma E \tag{5}$$

where ε and $\bar{\varepsilon}$ are the dielectric constants of the jet and the ambient air, respectively, E_n and E_t are the normal and tangential components of the electric field at the surface, and $\|*\|$ indicates the jump of a quantity across the surface of the jet. We have used the jump conditions for E_n and E_t: $\|\varepsilon E_n\| = \bar{\varepsilon}\overline{E_n} - \varepsilon E_n = \sigma$, $\|E_t\| = \overline{E_t} - E_t = 0$, and assumed that $\varepsilon E_n \approx \bar{\varepsilon}\overline{E_n}$ and $E_t \approx E$. The overbar indicates quantities in the surrounding air. The pressure $p(z)$ is determined by the radial momentum balance, and applying the normal force balance at the jet surface leads to:

$$-p + \tau_{rr} = t_n^e - \frac{\gamma}{R} \tag{6}$$

Inserting Equations (4)-(6) into Equation (3) yields (7):

$$\rho \upsilon \upsilon' = \rho g + \frac{3}{R^2}\frac{d}{dz}(\eta R^2 \upsilon') + \frac{\gamma R'}{R^2} + \frac{\sigma \sigma'}{\bar{\varepsilon}} + (\varepsilon - \bar{\varepsilon})EE' + \frac{2\sigma E}{R}$$

where η is the fluid viscosity and may depend on the local strain rate or the accumulated strain. The equation of electric field requires that:

$$E = E_\infty - \left[\frac{1}{\bar{\varepsilon}}(\sigma R)' - \left(\frac{\varepsilon}{\bar{\varepsilon}} - 1\right)\frac{(ER^2)''}{2}\right] ln\left(\frac{d}{R_0}\right) \tag{8}$$

where E_∞ is the applied external electric field, d is the distance between the nozzle and the collector, and R_0 is the radius of the spinneret.

CARBON NANOTUBE (CNT)

CNT structure

Carbon nanotubes are classified into single-walled nanotubes (SWNTs) and multi-walled nanotubes (MWNTs). A SWNT can be visualized as a graphene sheet that has been rolled into a hollow cylinder with end caps. So the atomic structure of SWNT can be described by the chiral vector C_h and the chiral angle θ (see Figure 5) given by:[70-77]

$$\vec{C_h} = n\vec{a_1} + m\vec{a_2} \tag{9}$$

where a_1 and a_2 are unit vectors and integers (n, m) are the number of steps along the zigzag carbon bonds. The tubes with n=m are known as armchair tubes and m=0 as zigzag tubes. In all other combinations of n and m, the SWNT are known as chiral tubes. Figure 6 illustrates the schematic of nanotubes with different chiralities, including armchair and zigzag nanotubes. The chiral angle θ is the angle made by the chiral vector C_h with respect to the zigzag direction (n, 0) and is defined as:

$$\theta = \cos^{-1}\frac{(2n+m)}{2\sqrt{(m^2+mn+n^2)}} \tag{10}$$

The radius of nanotube R is given by the following equation:

$$R = \frac{a\sqrt{(m^2+mn+n^2)}}{2\pi} \tag{11}$$

where a is a unit vector length and $a = a_{C-C}\sqrt{3}$, in which a_{C-C} is the carbon-carbon bond length and is equal to 0.1421 nm. Considering the effective wall thickness of SWNT t, the effective radius R_{eff} is defined as:

$$R_{eff} = \frac{a\sqrt{(m^2+mn+n^2)}}{2\pi} + \frac{t}{2} \tag{12}$$

To relate the graphene atomic coordinates and SWNT from a planer hexagonal lattice, the following equation is used:

$$(X, Y, Z) = [R\cos(\frac{x}{R}), R\sin(\frac{x}{R}), y] \quad (13)$$

where X, Y and Z represent the nanotube coordinates and x and y are the graphene coordinates. Table 1 summarizes the characteristic parameters of carbon nanotube.

CNT properties

It is well known that CNTs possess remarkable properties and have a combination of outstanding mechanical, electrical, thermal properties, and low density, so they have been suggested as excellent candidate for numerous applications.

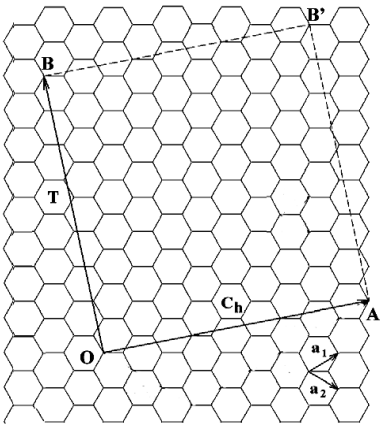

Figure 5: Schematic illustration of a hexagonal graphene sheet and definitions of SWNTs parameters

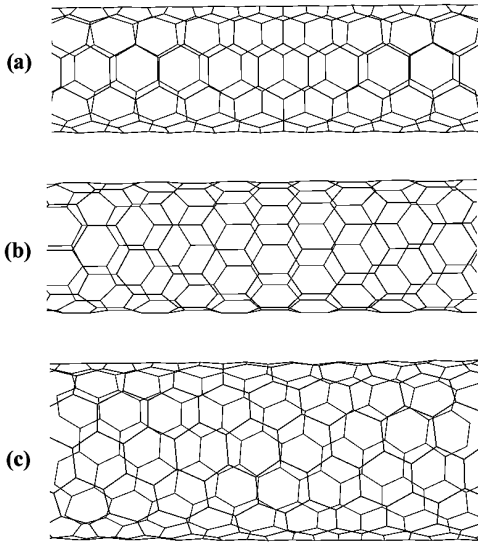

Figure 6: Schematic representation of (a) armchair (5,5), (b) zigzag (9,0), and (c) chiral (8,6) nanotubes

Table 1
Characteristic parameters of carbon nanotubes

Symbol	Description	Formula	Value
a_{C-C}	Carbon-carbon bond length	----	0.1421 nm
a	Unit vector length	$a = a_{C-C}\sqrt{3}$	0.2461 nm
a_1, a_2	Unit vectors	$\left(\frac{\sqrt{3}}{2}, \frac{1}{2}\right)a, \left(\frac{\sqrt{3}}{2}, -\frac{1}{2}\right)a$	in (x,y) coordinate system
C_h	Chiral vector	$C_h = n\,a_1 + m\,a_2$	(n, m) : integer
L	Circumference of nanotube	$L = \lvert C_h \rvert = a\sqrt{m^2 + mn + n^2}$	
R	Radius of nanotube	$R = \frac{a\sqrt{(m^2 + mn + n^2)}}{2\pi}$	
R_{eff}	Effective radius of nanotube	$R_{eff} = \frac{a\sqrt{(m^2 + mn + n^2)}}{2\pi} + \frac{t}{2}$	

θ	Chiral angle	$\theta = \cos^{-1}\frac{(2n+m)}{2\sqrt{(m^2+mn+n^2)}}$ $\theta = \sin^{-1}\frac{\sqrt{3}m}{2\sqrt{(m^2+mn+n^2)}}$ $\theta = \tan^{-1}\frac{\sqrt{3}m}{2n+m}$	$0° \le \theta \le 30°$

Table 2
Physical properties of CNTs

Physical property	Unit	CNT	
		SWNT	MWNT
Aspect ratio	----	100-10000	100-10000
Specific gravity	(g/cm^3)	0.8	1.8
Specific surface area	(m^2/g)	10-20	----
Elastic modulus	(GPa)	~ 1000	300-1000
Tensile strength	(GPa)	5-500	10-60
Thermal stability in air	(°C)	>600	>600
Thermal conductivity	(W/mK)	3000-6000	2000
Electrical conductivity	(S/cm)	10^2-10^6	10^3-10^5
Electrical resistivity	(μΩ/cm)	5-50	----

Some of these physical properties are summarized in Table 2.[78-80]

It is claimed that CNTs are a hundred times stronger than steel and have very high Young's modulus, which are the most important parameters that define the mechanical stiffness of a material. The actual measurements of CNT mechanical properties were made on individual arc discharge MWNTs using atomic force microscope (AFM). Young's modulus values of 270-970 GPa were obtained for a range of MWNTs.[81] The measurements on SWNT showed a tensile modulus of ~1000 GPa for small diameter SWNT bundles by bending methods. However, the properties of larger diameter bundles were dominated by shear slippage of individual nanotubes within the bundle.[25]

In addition to their outstanding mechanical properties, CNTs exhibit exceptionally high thermal and electrical conductivity. However, several parameters affect these properties, including the synthesis methods employed, defects, chirality, degree of graphitization and diameter.[82] For example, depending on chirality, the CNT can be metallic or semiconducting. The remarkable thermal conductivity of CNTs makes them particularly attractive for thermal management in composites. It is known that the thermal properties of CNTs play critical roles in controlling the performance of CNT based composite materials. Similarly, CNTs possess high electrical properties, which suggest their use in miniaturized electronic components.[83-85]

ELECTROSPUN CNT-POLYMER COMPOSITES

The incorporation of CNT into polymer matrix, due to the exceptional properties and large aspect ratio, has been proven to be a promising approach leading to structural materials and composites with excellent physical and mechanical properties, such as tensile strength, tensile modulus, strain to failure, torsional modulus, compressive strength, glass transition temperature, solvent resistance, and reduced shrinkage.[86] Fibrous materials were found to be most suitable for many applications. There are various techniques for the fabrication of CNT-polymer composites, such as solution casting, melt processing, melt spinning, electrospinning, and in-situ polymerization.[31] Electrospinning as an effective processing method to produce CNT-polymer nanofibers with the CNTs orienting to the axes of the as-spun nanofibers have attracted increasing attention during the last two decades.

Basic principles

As the alignment of CNTs in the polymer matrix is an interesting field, and has an important influence on unidirectional properties such as

strength, modulus, and toughness, electrospinning has been widely used to make CNTs align along the fiber axis. Due to the improved CNT alignment within the nanofibers and simple spinning process, this technique has been regarded as the most promising approach for producing electrospun carbon nanotube-polymer composites.[69,87] In this technique, initially the CNTs are randomly oriented, but they are aligned with the flow of polymer (see Figure 7). The CNT alignment has been analyzed based on the planar sink flow in a wedge, also known as Hamel flow.[88] This model implies that gradual alignment of random CNTs into the fiber occurs at the central streamline of the Taylor cone. While the nanotube center moves along the streamline, they are drawn towards the tip of the wedge.[89]

A number of reports on electrospun composite fibers using various types of polymers and CNTs are listed in Table 3. Although CNTs have potential to be embedded into various polymer matrices, electrospinning of some polymers causes difficulties.

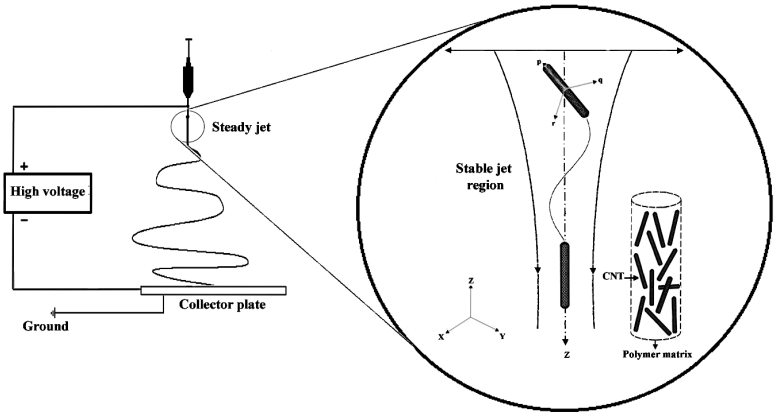

Figure 7: Schematic illustration of CNT alignment in jet flow

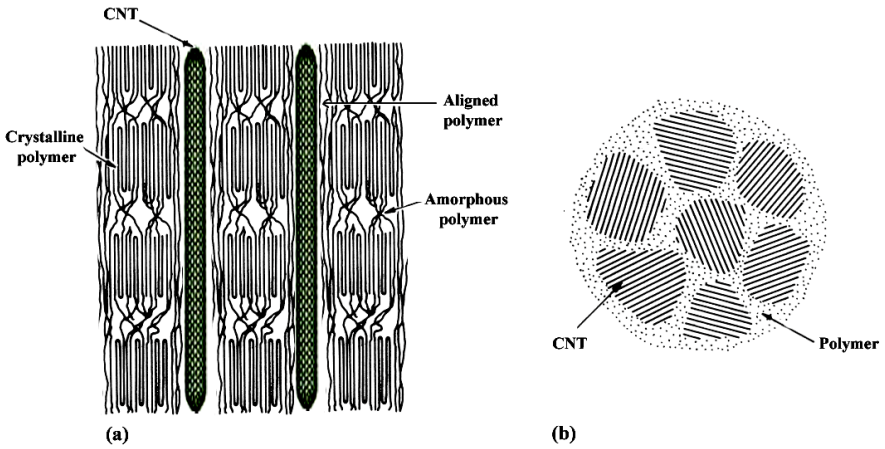

Figure 8: (a) Longitudinal and (b) cross-sectional representation of CNT-polymer composite fiber

Table 3
Electrospun CNT-polymer composites in the literature

Type of CNTs	Polymers	Molecular weight (M_w)	Solvents	CNTs (wt%)	Focus of the research	Ref.
SWNT	PVA	146000–186000, (96% hydrolyzed)	---	10	Structure-property relationships	[37]
MWNT	PVA	89000–98000, (99+% hydrolyzed)	Water/ethanol (3:1)	4	Effect of carbon nanotube aspect ratio and loading on elastic modulus	[90]
MWNT	PVA	75000-79000 (98-99% hydrolyzed)	Water	20 (v/v)%	Morphology and mechanical properties	[91]
MWNT	PTh	----	Chloroform	----	Electric and dielectric properties	[92]
MWNT	PAN	----	DMF	0.25	Effect of conductive additive and filler on the process	[93]
MWNT	PAN	----	DMF	0-10	Anisotropic electrical conductivity	[94]
MWNT	PAN	70000	DMF	2	Application of vibration technology in electrospinning	[95]
MWNT	PAN	150000	DMF	1	Monitoring the interaction between the π-electrons of CNT and the nitrile groups of PAN by using synchrotron microbeam WAXD analysis	[96]
MWNT	PAN	----	DMF	1	Creation of continuous yarn and characterization of the surface morphology, and the mechanical properties	[97]
SWNT	PAN/ MA/ itaconic acid (93:5.3:1.7w/w)	100000	DMF	0-1	Thermal and tensile properties	[98]
MWNT	PAN/ MA/ itaconic acid (93:5.3:1.7w/w)	100000	DMF	0-3	Investigating the distribution and alignment of CNT	[99]
MWNT	PMMA	350000	DMF	5	Tensile mechanics	[100]
SWNT	PMMA	996000	chloroform	0-1	Temperature dependent electrical resistance and morphology	[101]
MWNT	Poly(ε-caprolactone)	~ 100000	DMF	3	Effects of green tea polyphenols (GTP) and MWNTs incorporation on nanofiber morphology, mechanics, in vitro degradation and in vitro GTP release behaviors	[102]
MWNT	PS	185000	DMF/THF (2:3)	0.8, 1.6	Production of hollow nanofibers with un-collapsing and surface-porous structure	[103]
SWNT,	PS	----	DMF	0-5	Morphology, structure and properties	[42]

DWNT, MWNT						
MWNT	PLA	180000	DMF	1-5	Electrical conductivity, mechanical properties and in vitro degradation stability	[104]
SWNT	PLA/PAN	----	DMF	----	Fabrication of continuous CNT-filled nanofiber yarn	[35]
MWNT	PLLA/PCL	100000	Chloroform/ methanol (≈3:1)	0-3.75	Morphology, mechanical properties, in vitro degradation and biocompatibility	[105]
MWNT	PCL	----	Chloroform/ methanol (3:1)	2-3	Morphology and structural properties	[106]
MWNT	PC	----	----	15	Characterizing the composite nanofibers with directly embedded CNTs, with respect to the orientation and uniform dispersion of CNTs within the electrospun fibers	[107]
CNT	Alginate	----	Water	0-1	Mechanical and electrical properties	[43]
MWNT	PET	19200	TFA	0-3	Tensile, thermal, and electrical properties	[108]
MWNT	PA 6,6	----	FA/DCM (2:1)	0-2.5	Effect of fiber diameter on the deformation behavior of self-assembled electrospun CNT-PA 6,6 fibers	[109]
MWNT	PVDF/PPy	----	DMAc	1	Morphology, chemical structure, electrical conductivity, mechanical and thermal properties	[110]
MWNT	PEO	900000	Ethanol/water (40:60)	50 (v/v)%	Morphology and mechanical properties	[91]
MWNT	PANi/PEO	PANi=65000 PEO=600000	Chloroform	----	Electromagnetic interference shielding	[111]
MWNT	PANi/PEO	PANi=65000 PEO=100000	Chloroform	0.25-1	Electrical conductivity	[112]
MWNT	PPy	----	----	15	Electrochemistry and current-voltage characteristics	[113]
MWNT	PBT	----	HFIP	5	Morphology and mechanical properties	[114]

Acronyms: DWNT: Double-walled nanotube; PVA: Poly(vinyl alcohol); PTh: Poly(thiophene); PAN: Poly(acrylonitrile); MA: Methyl acrylate; PMMA: Poly(methyl methacrylate); PS: Polystyrene; PLA: Poly-DL-lactide; PC: Polycarbonate; PCL: Polycaprolactone; PET: Poly(ethylene terephthalate); PA: Polyamide; PVDF: Polyvinylidene fluoride; PPy: Polypyrrole; P(VDF-TrFE): Poly(inylidene difluoride-trifluoroethylene); PANi: Polyaniline; PEO: Poly(ethylene oxide); PU: Polyurethane; PBT: Poly(butylene terephthalate); DMF: *N,N*-dimethylformamide; THF: Tetrahydrofuran; TFA: Trifluoro acetic acid; FA: Formic acid; DCM: Dichloromethane; DMAc: *N,N*-dimethylacetamide; HFIP: Hexafluoro-2-propanol

* The molecular weight of the polymer is an estimate from literature. Also, where not specified, the average molecular weight is M_w

Structural and morphological properties

It has been found that most semi-crystalline polymers could be crystallized during the fiber formation process. During the electrospinning process, a fraction of the polymer chains crystallizes into lamellae or small crystallites, and another fraction remains amorphous.[5] The relaxed amorphous tie molecules exist between the crystalline parts of the chain. Figure 8 represents the expected general structure in CNT-polymer composite fiber.

Due to the shear and elongation forces acting on the jet, the tie molecules pass through the neighboring crystallites to form small-sized bundles and the lamellae are rearranged to form fibrils.[115] The crystalline and amorphous fractions of the chains within the electrospun fibers influence the physical and mechanical properties of the nanofibers.

The amorphous phase corresponds to the elastomeric properties and the crystalline phase provides dimensional stability. It seems that the CNTs embedded in electrospun fibers reduce the overall mobility of the polymer chains. Thus, the orientation of polymer chains during electrospinning and the presence of CNTs within the fibers enhance the structural properties of the electrospun CNT-polymer composite.[86]

It is known that rapid solvent evaporation from the electrospinning jet is accompanied by rapid structure formation and leads to a decrease in the jet temperature. Therefore, the aligned molecules have less time to realign themselves along the fiber axis, leading to less developed structure in the fiber.

There are two methods to study the morphological properties of electrospun CNT-polymer composites: one is electron microscopy (EM) and the second one is atomic force microscopy (AFM). As mentioned earlier, the final morphologies of the electrospun CNT-polymer composite fibers can be affected by several characteristics of the initial solution, such as solution concentration, CNT weight fraction, viscosity, surface tension and conductivity of solution, in addition to some electrospinning process (applied voltage, spinning distance, volume flow rate, and the strength of the applied electric field) and environmental conditions (temperature and humidity).

MECHANICAL PROPERTIES OF ELECTROSPUN CNT-POLYMER COMPOSITES

Background

The exceptional structure of CNTs, their low density, their high aspect ratio, and outstanding mechanical and physical properties make them an ideal candidate for specific applications in which CNTs are used as reinforcements in composite materials. There are several parameters that affect the mechanical properties of composite materials, including large aspect ratio of reinforcement, good dispersion, alignment and interfacial stress transfer.[80,82] These factors are discussed below.

The CNT aspect ratio is one of the main effective parameters on the longitudinal elastic modulus. Generally, the CNTs have a high aspect ratio, but their ultimate performance in a polymer composite is different. Stress transfer from the polymer matrix to the dispersed CNTs increases with the increase in the aspect ratio of CNTs.[116] However, the aggregation of CNTs could lead to a decrease in the effective aspect ratio of the CNTs.

The uniformity and stability of nanotube dispersion in a polymer matrix are probably the most fundamental issue for the performance of composite materials. A good dispersion and distribution of CNTs in the polymer matrix minimizes the stress concentration centers and improves the uniformity of stress distribution in the composites.[80] On the other hand, if the nanotubes are poorly dispersed within the polymer matrix, the composite will fail because of the separation of the nanotube bundle rather than the failure of the nanotube itself, resulting in significantly reduced strength.[117] Mazinani *et al*. studied the CNT dispersion for electrospun composite fiber, as well as its effect on the morphologies and properties of electrospun CNT-polystyrene nanocomposites.[42] They demonstrated that the CNT dispersion is an important controlling parameter for final fibers' diameter and morphology.

Another parameter influencing the mechanical properties of nanotube composites is the CNT alignment. The effects of CNT alignment on electrical conductivity and mechanical properties of CNT-polymer nanocomposites have been discussed in a number of researches.[118-120] For example, it has been reported that with increasing CNT alignment, the electrical and mechanical properties of the SWNT-epoxy composites

increased due to an increased interface bonding of CNTs in the polymer matrix.[119]

A good interfacial adhesion between the matrix and the nanotubes is another effective parameter of CNT-polymer composites. There are some possible adhesions between CNT and polymer matrix, including physical, chemical and/or mechanical. It is known that diffusive and electrostatic adhesions are not common in polymer composites. One of the most common types of adhesion in polymer composites is physical adhesion, such as van der Waals force, which refers to the intermolecular forces between CNT and polymer matrix. Chemical adhesion as the strongest form of adhesion represents chemical bonding between the CNT and polymer matrix. The interlocking and entanglement of CNT functional chains and polymer matrix can be represented by mechanical adhesion. It should be mentioned that nanotubes and nanofibers due to their perfect cylinders with smooth surface exhibit insignificant mechanical interlocking with the polymer matrix.[80]

Other parameters influencing the mechanical properties of nanotube composites include: solvent selection, size, crystallinity, crystalline orientation, purity, entanglement, and straightness.[82]

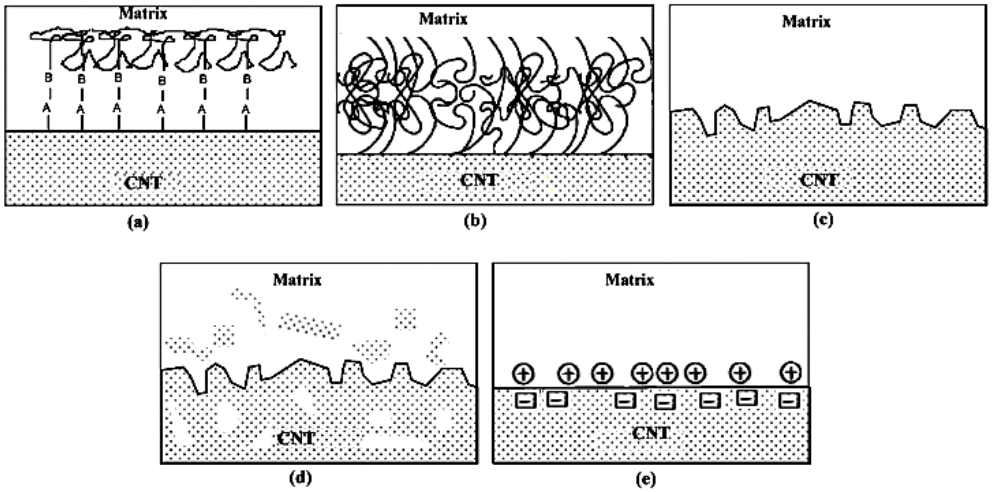

Figure 9: Schematic representation of (a) chemical bonding, (b) molecular entanglement, (c) mechanical interlocking, (d) diffusion adhesion, and (e) electrostatic adhesion between the matrix and the CNTs

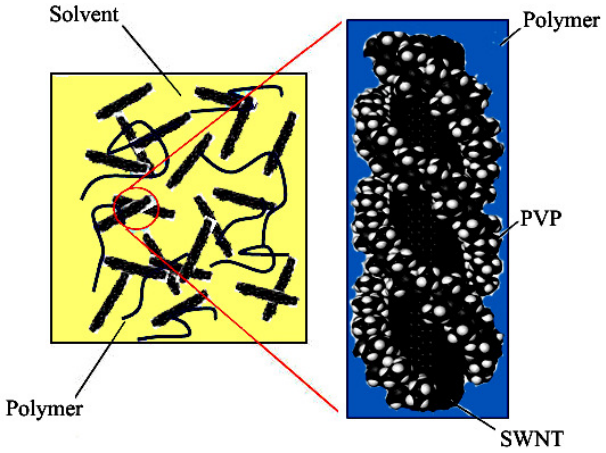

Figure 10: Schematic representation of functionalized CNT

CNT-polymer interactions

In CNT-polymer composites, the constituents retain their own original chemical and physical identities, but together they produce a combination of properties that cannot be achieved by any of the components acting alone.[121] The properties of composite materials greatly depend on the nature of the bonding at the interface, the mechanical load transfer from the surrounding matrix to the nanotube and the strength of the interface. The interface plays an important role in optimizing load transfer between the CNT and the polymer matrix. The mechanism of interfacial load transfer from the matrix to nanotubes can be categorized as: micromechanical interlocking, chemical bonding, and the weak van der Waals force between the matrix and the reinforcement.[122,123] As reported previously, if the load stress cannot be effectively transferred from the matrix to the CNTs, the physical and mechanical properties of the nanocomposites could be considerably lower than the expected. In order to improve the mechanical properties of nanocomposite materials, strong interfacial interaction between the nanotubes and the polymer matrix is a necessary condition, but might not be a sufficient condition.

In addition to interfacial interactions between the CNT and the polymer matrix, the dispersion of CNTs in the polymer has significant influence on the performance of a CNT-polymer nanocomposite. Many different approaches have been used by researchers in an attempt to disperse CNT in the polymer matrix, such as physical sonication and chemical modification of CNT surface.[124-126] Functionalization of CNT surface can lead to the construction of chemical bonds between the nanotube and the polymer matrix and offers the most efficient solution for the formation of a strong interface. A strong interface between the coupled CNT-polymer creates an efficient stress transfer.[31] It should be noted that covalent functionalization of CNT may disrupt the graphene sheet bonding, and thereby reduce the mechanical properties of the final product. However, non-covalent treatment of CNT can improve the CNT-polymer composite properties through various specific interactions.[127]

Measurements

According to the literature, most studies on CNT-polymer composites have reported the enhancement of mechanical strength by CNT addition, and this is of particular importance for electrospun nanofibers. It is well known that measuring the mechanical properties of individual electrospun nanofibers is difficult due to the small size. In this regard, a few experimental investigations reported their findings on measuring the mechanical properties of single electrospun composite nanofiber.[128-132]

Several nanomechanical characterization techniques have been suggested to measure the elastic properties of individual electrospun nanofibers, such as AFM cantilevers, universal tensile tester, and AFM-based nanoindentation system.[133,134] Among them, AFM-based techniques have been widely used to measure the mechanical properties of single electrospun nanofibers. This technique was carried out by attaching nanofiber to two AFM cantilever tips and recording the cantilever resonances for both the free cantilever vibrations and for the case where the microcantilever system has nanofibers attached. Young's modulus of the nanofiber is then derived from the measured resonant frequency shift resulting from the nanofiber. A similar experiment has been carried out for electrospun polyethylene oxide (PEO) nanofibers[130] by using a piezo-resistive AFM tip. In this work, the selected nanofiber was first attached to a piezo-resistive AFM cantilever tip and to a movable optical microscope stage. The nanofiber was stretched by moving the microscope stage and the force applied to the nanofiber was measured via the deflection of the cantilever. These techniques are suitable for fibers with the diameter ranging from several micrometers to tens of nanometers. However, it is difficult to manipulate and test individual nanofibers.[133]

ELECTROSPUN CNT-POLYMER COMPOSITE APPLICATIONS

The research and development of electrospun nanofibers has evinced more interest and attention in recent years due to the enhanced awareness of its potential applications in the medical, engineering and defence fields.[135-140] Despite the several published reviews on polymer nanofiber applications, few investigations have been reported on the applications of electrospun CNT-polymer composites. Most of the works on electrospun CNT-polymer composite fibers have

focused on developing a fundamental understanding of the composite structure-property relationships.

Electrospun CNT-polymer composite nanofibers, due to their excellent mechanical, thermal, and electrical properties, as well as nanometer scale diameter, are appropriate for a large variety of potential applications, such as in military protective clothing, in fuel cells, in nanosensors and in energy storage. Figure 11 shows the potential applications of electrospun composite nanofibers.[140-146]

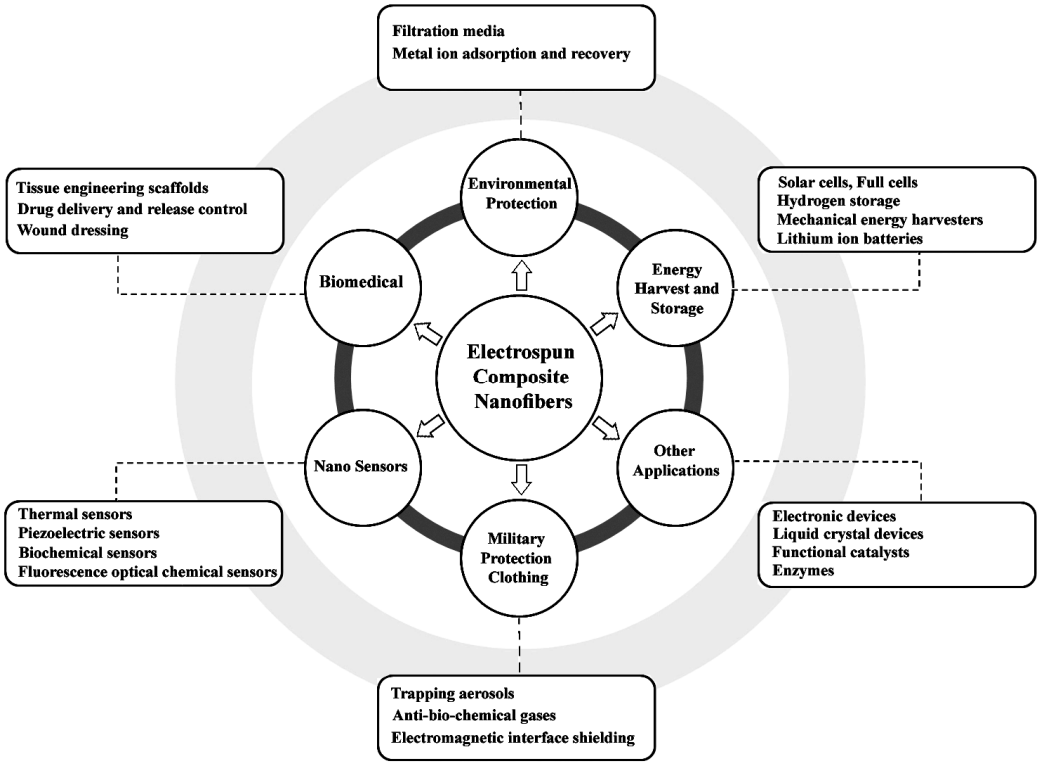

Figure 11: Potential applications of electrospun composite nanofibers

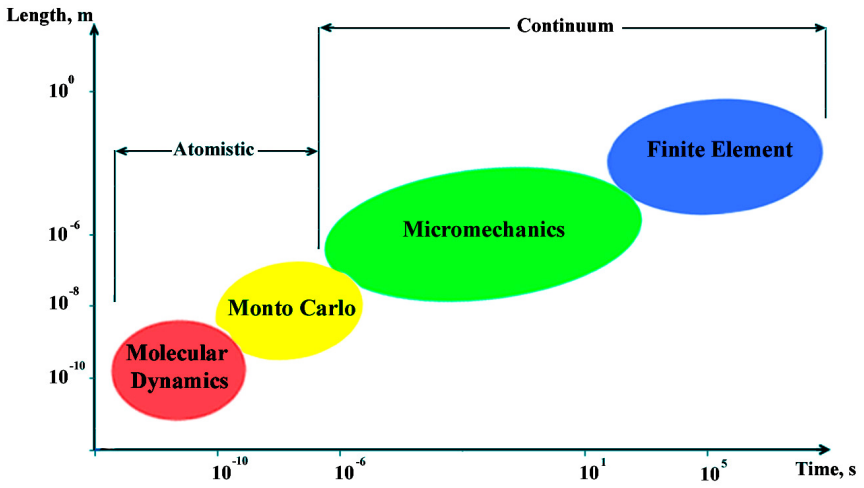

Figure 12: Range of different length and time scales and theoretical approaches; adapted from Shokrieh *et al.*[46]

In a recent investigation, electrospun chitosan/PVA nanofibers reinforced by SWNT (SWNT-CS/PVA) have been used as scaffold for neural tissue engineering.[147] The *in vitro* biocompatibility of the electrospun fiber mats was also assessed using human brain-derived cells and U373 cell lines. The obtained results indicated that SWNTs as reinforcing phase can augment the morphology, porosity, and structural properties of CS/PVA nanofiber composites and thus benefit the proliferation rate of both cell types. Moreover, the cells exhibit their normal morphology while integrating with surrounding fibers.[147] In another study, electrospun MWNT-PANi/PEO nanofibers were found to enhance the electromagnetic interface (EMI) shielding properties of nanofibers.[148] It was found that absorption was the main reaction that shielded the electromagnetic interference. Electrospun CNTs-polymer nanofibers have also shown potential applications in filter media, tissue engineering scaffolds, wound dressing, face masks, drug delivery, enzyme carriers, super capacitors, and composite reinforcement.[135, 149-151]

THEORETICAL APPROACHES TO CNT-POLYMER COMPOSITES

Background

Due to the difficulties encountered in the experimental characterization of nanomaterials, theoretical approaches to determining the CNT-based composite properties have attracted a great interest. A tremendous amount of research has been developed to understand the mechanical behavior of CNTs and their composites. According to the literature, the theoretical and computational approaches can be mainly classified into two categories: i) atomistic modeling, and ii) continuum mechanics approaches[152-164] (see Figure 12).

The atomistic modeling technique includes three important categories, namely the molecular dynamics (MD), Monte Carlo (MC), and *ab initio* approaches. The MD and MC simulations are constructed using Newton's second law and the *ab initio* approach relies on the accurate solution of the Schrödinger equation to extract the locations of each atom. Tight bonding molecular dynamics (TBMD), local density approximation (LDA), and density functional theory (DFT) are other combined approaches, which are often computationally expensive.[46] Although the atomistic modeling technique provides a valuable insight into complex structures, due to its huge computational effort especially for large-scale CNTs with high number of walls, its application is limited to the systems with a small number of atoms. Therefore, the alternative continuum mechanics approaches were proposed for larger systems or larger time. Figure 12 shows the range of different length and time scales with the corresponding theoretical approaches.

Continuum mechanics based approach is considered as an efficient way to save computational resources. This technique employs the continuum mechanics theories of shells, plates, beams, rods and trusses. The continuum mechanics approach by establishing a linkage between structural mechanics and molecular mechanics has aroused widespread interest. Recently, some studies have been developed based on continuum mechanics for estimating elastic properties of CNTs. For instance, Odegard *et al*.[165] and Li and Chou[166] developed a molecular structural mechanics approach for modeling CNTs. The finite element (FE) method has been recently introduced to describe the mechanical properties of CNTs. In this regard, Tserpes and Papanikos[153] proposed a FE model for SWNTs. By using a linkage between molecular and continuum mechanics, they determined the elastic moduli of beam element. Furthermore, they reported the dependence of elastic modulus on the diameter and chirality of the nanotubes.

It should be noted that the results obtained from these approaches might be higher than those observed in experiments. This may be due to the idealized conditions that are assumed, especially the perfect bonding conditions at the CNT-polymer interfacial region. Table 4 shows a comparison of experimental and theoretical results for Young's modulus of SWNT. These theoretical Young's modulus ranges approximately agree with the experimental measurements for the SWNT studied.

Summary of literature data

Nowadays modeling and simulation of CNTs-polymer composites is of special interest to many researchers. For example, Shokrieh and Rafiee[193] compared the results of finite element (FE) analysis and the rule of mixture and deduced that the latter overestimates the properties of the investigated composite and leads to inappropriate

results. This observation is in agreement with that of other researchers.[194-198] The effects of CNT aspect ratio, CNT volume fraction, and matrix modulus on axial stress and interfacial shear stress were studied by Haque and Ramasetty.[199] Xiao and Zhang[200] employed the Cox model to investigate the effects of the length and the diameter of the CNTs on the distributions of the tensile and interfacial shear stress of SWNTs in an epoxy matrix.

Eken *et al*.[201] studied the combined effects of nanotube aspect ratio and shear rate on the electrical properties and microstructure of CNT-polymer composite. They presented that the orientation of the nanotubes and electrical properties of the CNT-polymer composites strongly depend on the nanotube aspect ratio and applied shear rate.

Table 4
Comparison between different theoretical and experimental results of SWNT Young's modulus

	Method	Wall thickness (nm)	Young's modulus (GPa)	Ref.
Theoretical approaches	MD	----	1100-1200	[167]
	MD	0.066	5500	[168]
	MD, force approach (FA)	----	1350	[169]
	MD, energy approach (EA)	----	1238	[169]
	ab initio	----	750-1180	[170]
	ab initio	0.089	3859	[171]
	TBMD	0.34	1240	[172]
	TBMD	----	5100	[173]
	DFT	----	1240	[174]
	Molecular mechanics	----	1325	[175]
	MD, Brenner potential	----	5500	[176]
	Nanoscale continuum	----	4750-7050	[177]
	LDA combined with elastic shell theory	0.075	4700	[178]
	Molecular structural mechanics model	0.34	Z: 1080±20; A: 1050±20	[179]
	Continuum mechanics model	0.0617	4480	[180]
	Analytical molecular structural mechanics based on the Morse potential	----	1000-1200	[181]
	Energy equivalence between truss and chemical models	----	2520	[182]
	Combined FEM and continuum mechanics, elastic shell	----	4840	[183]
	Structural mechanics approach, space frame, stiffness matrix method	----	1050	[166]
	Molecular mechanics-based FEM, elastic rod element	----	400	[184]
	Space frame and beam	----	9500-1060	[153]
	Beam element and nonlinear spring	----	9700-1050	[185]
	Spring elements	----	1080-1320	[71]
Experimental	3-D beam element	----	400-2080	[186]
	Thermal vibrations-TEM	----	400-4150	[187]
	Cooling-induced vibrations, micro-Raman spectroscopy	----	2800-3600	[188]
	Measuring resonance frequency	----	Z: 100-1000	[189]
	Tensile test-AFM	----	1002	[190]
	3-point bending-AFM	----	1200	[191]
	TEM	----	Z: 900-1700	[192]

MD: Molecular dynamics; TBMD: Tight bonding molecular dynamics; DFT: Density functional theory; LDA: Local density approximation; FEM: Finite element method; TEM: Transmission electron microscope; AFM: Atomic force microscope; [a] Z: Zigzag; [b] A: Armchair

Georgantzinos *et al*.[202] carried out multi-scale FE formulation to investigate the stress-strain behavior of rubber uniformly filled with continuous SWNTs. They concluded that the SWNTs improve significantly the composite strength and toughness especially for higher volume fractions. A molecular structural mechanics model of CNT-reinforced composites has been proposed by Wang *et al*.[203] It is assumed that CNTs and matrix are perfectly bonded to each other. They also presented the effects of matrix materials, van der Waals force, chiral vector, and tube layers of CNTs on interfacial stresses in CNT-reinforced composites. In the study on multi-scale modeling of CNT-reinforced nanofiber scaffold by Unnikrishnan *et al*.,[204] it was demonstrated that the CNT polymeric scaffold properties estimated using both the micromechanical and nonlinear hyperelastic material homogenization models were in excellent agreement with experimental data. In another study, mechanical performance of CNT-reinforced polymer composites at cryogenic temperatures was performed experimentally and numerically by Takeda *et al*.[205] FE computations were used to model the representative volume element (RVE) of the composites, and the possible existence of the imperfect CNT-polymer interface bonding was considered. Joshi *et al*.[164] implemented the continuum mechanics approach using a hexagonal RVE under lateral loading conditions to investigate the mechanical properties of CNT reinforced composite. They also used an extended rule of mixtures (ERM) to validate the proposed model. The reported theoretical approaches on mechanical properties of CNT-polymer composites, including corresponding validation technique and interface bonding, are given in Table 5.

Table 5
Theoretical approaches to predicting the mechanical properties of CNT-polymer composites[46]

Theoretical approaches	Validation technique	SWNT in matrix		Interface bonding
		Single	Disperse	
Equivalent continuum mechanics	Mechanical testing	×	✓	Perfect
FEM, strain energy method	Literature data	×	✓	Perfect
MD, energy minimization method	Rule of mixture	✓	×	Perfect
MD, Brenner and united-atom potential	Ordinary and extended rule of mixture	✓	×	Perfect
Combined FEM and micromechanics models (wavy and straight SWNTs)	Literature data	×	✓	Perfect
Square RVE, FEM, rule of mixture, and elasticity theory	Consistent with some experimental data	×	✓	Perfect
Micromechanics equations for randomly oriented short fibers	Experimental	×	✓	Perfect
Multiscale Monte Carlo FEM using the equivalent continuum method	Tensile test at the macroscale	×	✓	Perfect
FEM, strain energy method	Literature data	×		Perfect
Beam elements for SWCNTs using molecular structural mechanics, truss rod for vdW links, cubic elements for matrix	-----	✓	×	vdW interaction

vdW: van der Waals

CONCLUDING REMARKS AND FUTURE WORK

CNTs have emerged as promising reinforcements for polymer composites due to their high aspect ratios and exceptionally remarkable mechanical properties. Studies have shown that the mechanical properties of CNT-polymer composites are affected by many parameters, including type of CNTs, chirality, purity, aspect ratio, loading content, dispersion, alignment and interfacial adhesion between the CNT and polymer matrix. Among them, the interfacial adhesion is identified as one of the most important factors affecting the performance of nanocomposites.

The introduction of CNTs into electrospun polymer nanofibers is an interesting attempt to enhance the mechanical properties of electrospun CNT-polymer composite nanofibers. So far, a few reports have been found in the literature regarding

the measurement of the mechanical properties of single electrospun composite nanofiber. The isolation of individual composite nanofibers remains the biggest challenge in measuring the tensile properties of composite nanofibers, due to the small size of the samples. Another challenge is to grip it into a sufficiently small load scale tester. Although a number of studies have been performed on the experimental investigation of electrospun CNT-polymer composites, more attention should be given to the theoretical approaches on predicting the mechanical properties of CNTs embedded in electrospun fiber mat. Accordingly, this review summarizes recent results on modeling and simulation of CNT-polymer composites.

Along with the development of theoretical and computational approaches for nanotubes, many techniques have been demonstrated in many studies using atomistic modeling and continuum mechanics approaches. A molecular simulation through the atomistic approach, such as molecular dynamics or Monte Carlo, has been successfully used in materials science and engineering to determine the physical and mechanical properties of materials in nanoscale. One of the main challenges in applying such a simulation to a single electrospun composite nanofiber is the huge amount of computational tasks especially for a large number of atoms. Another challenge is to determine the structure and arrangement of nanofiber and also to establish an interatomic potential function.

REFERENCES

[1] A. K. Haghi and G. Zaikov, "Advances in Nanofiber Research", *i*Smithers, UK, 2011.

[2] J. Fang, X. Wang, T. Lin, in "Nanofibers-Production, Properties and Functional Applications", edited by T. Lin, InTech, 2011, pp. 287-326.

[3] D. Li and Y. Xia, *Adv. Mater.*, **16**, 1151 (2004).

[4] D. H. Reneker, and I. Chun, *Nanotechnology*, **7**, 216 (1996).

[5] A. Baji, Y. W. Mai, S. C. Wong, M. Abtahi, P. Chen, *Compos. Sci. Technol.*, **70**, 703 (2010).

[6] V. Mottaghitalab and A. K. Haghi, *Korean. J. Chem. Eng.*, **28**, 114 (2011).

[7] M. Ziabari, V. Mottaghitalab, A. K. Haghi in "Nanofibers: Fabrication, Performance, and Applications", edited by W. N. Chang, Nova Science Publishers, New York, 2009, pp. 153-182.

[8] S. L. Shenoy, W. D. Bates, H. L. Frisch and G. E. Wnek, *Polymer*, **46**, 3372 (2005).

[9] C. Burger, B. S. Hsiao and B. Chu, *Annu. Rev. Mater. Res.*, **36**, 333 (2006).

[10] A. K. Haghi and M. Akbari, *Phys. Status. Solid. A.*, **204**, 1830 (2007).

[11] K. Nasouri, H. Bahrambeygi, A. Rabbi, A. M. Shoushtari and A. Kaflou, *J. Appl. Polym. Sci.*, **126**, 127 (2012).

[12] T. Subbiah, G. S. Bhat, R. W. Tock, S. Parameswaran and S. S. Ramkumar, *J. Appl. Polym. Sci.*, **96**, 557 (2005).

[13] M. Hasanzadeh, B. Hadavi Moghadam, in "Research Progress in Nanoscience and Nanotechnology", edited by A. K. Haghi, Nova Science Publisher, New York, 2012, pp. 47-70.

[14] J. H. Park, B. S. Kim, Y. C. Yoo, M. S. Khil and H. Y. Kim, *J. Appl. Polym. Sci.*, **107**, 2211 (2008).

[15] F. L. Zhou and R. H. Gong, *Polym. Int.*, **57**, 837 (2008).

[16] D. R. Nisbet, J. S. Forsythe, W. Shen, D. I. Finkelstein and M. K. Horne, *J. Biomater. Appl.*, **24**, 7 (2009).

[17] S. R. Bhattarai, N. Bhattarai, H. K. Yi, P. H. Hwang, D. I. Cha *et al.*, *Biomaterials*, **25**, 2595 (2004).

[18] W. J. Li, C. T. Laurencin, E. J. Caterson, R. S. Tuan and F. K. Ko, *J. Biomed. Mater. Res.*, **60**, 613 (2002).

[19] H. Lu, W. Chen, Y. Xing, D. Ying and B. Jiang, *J. Bioact. Compat. Pol.*, **24**, 158 (2009).

[20] S. Lee and S. K. Obendorf, *Text. Res. J.*, **77**, 696 (2007).

[21] T. L. Sill and H. A. von Recum, *Biomaterials*, **29**, 1989 (2008).

[22] C. Kim, *J. Power. Sources*, **142**, 382 (2005).

[23] C. Kim, B. T. N. Ngoc, K. S. Yang, M. Kojima, Y. A. Kim *et al.*, *Adv. Mater.*, **19**, 2141 (2007).

[24] V. Thavasi, G. Singh and S. Ramakrishna, *Energ. Environ. Sci.*, **1**, 205 (2008).

[25] J. P. Salvetat, G. A. D. Briggs, J. M. Bonard, R. R. Bacsa, A. J. Kulik *et al.*, *Phys. Rev. Lett.*, **82**, 944 (1999).

[26] T. W. Ebbesen, H. J. Lezec, H. Hiura, J. W. Bennett, H. F. Ghaemi *et al.*, *Nature*, **382**, 54 (1996).

[27] S. Berber, Y. K. Kwon and D. Tomanek, *Phys. Rev. Lett.*, **84**, 4613 (2000).

[28] H. Dai, *Surf. Sci.*, **500**, 218 (2002).

[29] I. Kanga, Y. Y. Heung, J. H. Kim, J. W. Lee, R. Gollapudi *et al.*, *Compos. Part B-Eng.*, **37**, 382 (2006).

[30] J. P. Salvetat-Delmotte and A. Rubio, *Carbon*, **40**, 1729 (2002).

[31] M. Naebe, T. Lin, X. Wang, in "Nanofibers", edited by A. Kumar, InTech, 2010, pp. 309-328.

[32] V. Choudhary, A. Gupta, in "Carbon Nanotubes-Polymer Nanocomposites", edited by S. Yellampalli, InTech, 2011, pp. 65-90.

[33] J. Gao, A. Yu, M. E. Itkis, E. Bekyarova, B. Zhao *et al.*, *J. Am. Chem. Soc.*, **126**, 16698 (2004).

[34] I. S. Chronakis, *J. Mater. Process. Tech.*, **167**, 283 (2005).

[35] F. Ko, Y. Gogotsi, A. Ali, N. Naguib, H. Ye *et al*., *Adv. Mater*., **15**, 1161 (2003).
[36] M. Naebe, T. Lin, W. Tian, L. Dai and X. Wang, *Nanotechnology*, **18**, 1 (2007).
[37] M. Naebe, T. Lin, M. P. Staiger, L. Dai, X. Wang, *Nanotechnology*, **19**, 305702 (2008).
[38] G. Mathew, J. P. Hong, J. M. Rhee, H. S. Lee, C. Nah, *Polym. Test*., **24**, 712 (2005).
[39] K. Nasouri, A. M. Shoushtari, A. Kaflou, H. Bahrambeygi, A. Rabbi, *Polym. Compos*., **33**, 1951 (2012).
[40] Z. M. Mahdieh, V. Mottaghitalab, N. Piri, A. K. Haghi, *Korean J. Chem. Eng*., **29**, 111 (2012).
[41] V. Mottaghitalab, A. K. Haghi, in "Development of Nanotechnology in Textiles", edited by A. K. Haghi, and G. E. Zaikov, Nova Science Publisher, New York, 2012, pp. 11-88.
[42] S. Mazinani, A. Ajji and C. Dubois, *Polymer*, **50**, 3329 (2009).
[43] M. S. Islam, M. Ashaduzzaman, S. M. Masum, J. H. Yeum, *Dhaka Univ. J. Sci*., **60**, 125 (2012).
[44] Q. Zhang, Z. Chang, M. Zhu, X. Mo, D. Chen, *Nanotechnology*, **18**, 115611 (2007).
[45] H. Ye, H. Lam, N. Titchenal, Y. Gogotsi and F. Ko, *Appl. Phys. Lett*., **85**, 1775 (2004).
[46] M. M. Shokrieh and R. Rafiee, *Mech. Compos. Mater*., **46**, 155 (2010).
[47] A. Kilic, F. Oruc and A. Demir, *Text. Res. J*., **78**, 532 (2008).
[48] A. Shams Nateri and M. Hasanzadeh, *J. Comput. Theor. Nanosc*., **6**, 1542 (2009).
[49] M. Ziabari, V. Mottaghitalab and A. K. Haghi, *Korean J. Chem. Eng*., **27**, 340 (2010).
[50] M. Ziabari, V. Mottaghitalab and A. K. Haghi, *Braz. J. Chem. Eng*., **26**, 53 (2009).
[51] M. Ziabari, V. Mottaghitalab, S. T. McGovern, A. K. Haghi, *Chinese Phys. Lett*., **25**, 3071 (2008).
[52] M. Ziabari, V. Mottaghitalab, S. T. McGovern, A. K. Haghi, *Nanoscale Res. Lett*., **2**, 297 (2007).
[53] M. Ziabari, V. Mottaghitalab and A. K. Haghi, *Korean J. Chem. Eng*., **25**, 919 (2008).
[54] M. Ziabari, V. Mottaghitalab and A. K. Haghi, *Korean J. Chem. Eng*., **25**, 905 (2008).
[55] M. Ziabari, V. Mottaghitalab and A. K. Haghi, *Korean J. Chem. Eng*., **25**, 923 (2008).
[56] K. Nasouri, A. M. Shoushtari, A. Kaflou, *Micro. Nano. Lett*., **7**, 423 (2012).
[57] N. Sabetzadeh, H. Bahrambeygi, A. Rabbi, K. Nasouri, *Micro. Nano. Lett*., 7, 662 (2012).
[58] A. L. Yarin, S. Koombhongse, D. H. Reneker, *J. Appl. Phys*., **90**, 4836 (2001).
[59] J. Doshi and D. H. Reneker, *J. Electrostat*., **35**, 151 (1995).
[60] S. A. Theron, E. Zussman, A. L. Yarin, *Polymer*, **45**, 2017 (2004).
[61] D. H. Reneker, A. L. Yarin, H. Fong, S. Koombhongse, *J. Appl. Phys*., **87**, 4531 (2000).
[62] J. J. Feng, *Phys. Fluids*., **14**, 3912 (2002).
[63] C. P. Carroll, Y. L. Joo, *Phys. Fluids*., **18**, 053102 (2006).
[64] E. Zhmayev, H. Zhou, Y. L. Joo, *J. Non-Newton. Fluid Mech*., **153**, 95 (2008).
[65] J. J. Stanger, M. Sc. thesis, University of Canterbury, 2008.
[66] Y. M. Shin, M. M. Hohman, M. P. Brenner, G. C. Rutledge, *Polymer*, **42**, 9955 (2001).
[67] S. Zhang, W. S. Shim, J. Kim, *Mater. Design*, **30**, 3659 (2009).
[68] O. S. Yördem, M. Papila, Y. Z. Menceloğlu, *Mater. Design*, **29**, 34 (2008).
[69] A. Agic, *J. Appl. Polym. Sci*., **108**, 1191 (2008).
[70] M. Meo, M. Rossi, *Compos. Sci. Technol*., **66**, 1597 (2006).
[71] G. I. Giannopoulos, P. A. Kakavas, N. K. Anifantis, *Comp. Mater. Sci*., **41**, 561 (2008).
[72] T. Natsuki, K. Tantrakarn, M. Endo, *Appl. Phys. A*, **79**, 117 (2004).
[73] R. Ansari, S. Rouhi, *Physica E*., **43**, 58 (2010).
[74] D. Qian, G. J. Wagner, W. K. Liu, M. F. Yu, R. S. Ruoff, *Appl. Mech. Rev*., **55**, 495 (2002).
[75] J. M. Wernik, S. A. Meguid, *Appl. Mech. Rev*., **63**, 050801 (2010).
[76] T. Belin, F. Epron, *Mater. Sci. Eng. B*., **119**, 105 (2005).
[77] V. N. Popov, *Mater. Sci. Eng. R*., **43**, 61 (2004).
[78] M. H. Al-Saleh, U. Sundararaj, *Carbon*, **47**, 2 (2009).
[79] P. C. Ma, N. A. Siddiqui, G. Marom, J. K. Kim, *Compos. Part A-Appl. S*., **41**, 13451367 (2010)
[80] M. H. Al-Saleh, U. Sundararaj, *Compos. Part A-Appl. S*., **42**, 2126 (2011).
[81] J. N. Coleman, U. Khan, W. J. Blau, Y. K. Gun'ko, *Carbon*, **44**, 1624 (2006).
[82] Z. Moridi, V. Mottaghitalab, A. K. Haghi, *Cellulose Chem. Technol*., **45**, 549 (2011).
[83] R. Khare, S. Bose, *J. Miner. Mater. Charact. Eng*., **4**, 31 (2005).
[84] A. Chiolerio, M. Castellino, P. Jagdale, M. Giorcelli, S. Bianco *et al*., in "Carbon Nanotubes-Polymer Nanocomposites", edited by S. Yellampalli, InTech, 2011, pp. 215-230.
[85] O. Breuer, U. Sundararaj, *Polym. Compos*., **25**, 630 (2004).
[86] B. G. Min, H. G. Chae, M. L. Minus, S. Kumar, in "Functional Composites of Carbon Nanotubes and Applications", edited by K. P. Lee, A. L. Gopalan, F. D. S. Marquis, Transworld Research Network, India, 2009, pp. 43-73.
[87] A. Agic A, B. Mijovic, in "Engineering the Future", edited by L. Dudas, InTech, 2010, pp. 26-46.
[88] Y. Dror, W. Salalha, R. L. Khalfin, Y. Cohen, A. L. Yarin *et al*., *Langmuir*, **19**, 7012 (2003).
[89] L. Y. Yeo, J. R. Friend, *J. Exp. Nanosci*., **1**, 177 (2006).

[90] K. K. H. Wong, M. Zinke-Allmanga, J. L. Hutter, S. Hrapovic, J. H. T. Luong *et al*., *Carbon*, **47**, 2571 (2009).
[91] W. Zhou, Y. Wu, F. Wei, G. Luo, W. Qian, *Polymer*, **46**, 12689 (2005).
[92] D. C. Tiwari, V. Sen, R. Sharma, *Indian J. Pure Appl. Phys*., **50**, 49 (2012).
[93] P. Heikkilä, A. Harlin, *eXPRESS Polym. Lett*., **3**, 437 (2009).
[94] E. J. Ra, K. H. An, K. K. Kim, S. Y. Jeong, Y.H. Lee, *Chem. Phys. Lett*., **413**, 188 (2005).
[95] Y. Q. Wan, J. H. He, J. Y. Yu, *Polym. Int*., **56**, 1367 (2007).
[96] L. Vaisman, E. Wachtel, H. D. Wagner, G. Marom, *Polymer*, **48**, 6843 (2007).
[97] N. M. Uddin, F. Ko, J. Xiong, B. Farouk, F. Capaldi, *Res. Lett. Mater. Sci*., Doi: 10.1155/2009/868917 (2009).
[98] B. Qiao, X. Ding, X. Hou, S. Wu, *J. Nanomater*., Doi: 10.1155/2011/839462, (2011).
[99] J. Ji, G. Sui, Y. Yu, Y. Liu, Y. Lin *et al*., *J. Phys. Chem. C*., **113**, 4779 (2009).
[100] L. Q. Liu, D. Tasis, M. Prato, H. D. Wagner, *Adv. Mater*., **19**, 1228 (2007).
[101] B. Sundaray, V. J. Babu, V. Subramanian, T.S. Natarajan, *J. Eng. Fiber Fabr*., **3**, 39 (2008).
[102] S. Shao, L. Li, G. Yang, J. Li, C. Luo *et al*., *Int. J. Pharm*., **421**, 310 (2011).
[103] C. Pan, L. Q. Ge, Z. Z. Gu, *Compos. Sci. Technol*., **67**, 3271 (2007) .
[104] S. Shao, S. Zhou, L. Li, J. Li, C. Luo *et al*., *Biomaterials*, **32**, 2821 (2011).
[105] G. Y. Liao, X. P. Zhou, L. Chen, X. Y. Zeng, X. L. Xie *et al*., *Compos. Sci. Technol*., **72**, 248 (2012).
[106] K. Saeed, S. Y. Park, H. J. Lee, J. B. Baek, W. S. Huh, *Polymer*, **47**, 8019 (2006).
[107] G. M. Kim, G. H. Michler, P. Pötschke, *Polymer*, **46**, 7346 (2005).
[108] B. W. Ahn, Y. S. Chi, T. J. Kang, *J. Appl. Polym. Sci*., **110**, 4055 (2008).
[109] A. Baji, Y. W. Mai, S. C. Wong, *Mater. Sci. Eng. A*, **528**, 6565 (2011).
[110] K. Ketpang, J. S. Park, *Synthetic Met*., **160**, 1603 (2010).
[111] J. S. Im, J. G. Kim, S. H. Lee, Y. S. Lee, *Colloid. Surface A*, **364**, 151 (2010).
[112] M. K. Shin, Y. J. Kim, S. I. Kim, S. K. Kim, H. Lee *et al*., *Sensor Actuat. B-Chem*., **134**, 122 (2008).
[113] G. Han, G. Shi, *J. Appl. Polym. Sci*., **103**, 1490 (2007).
[114] G. Mathew, J. P. Hong, J. M. Rhee, H. S. Lee, C. Nah, *Polym. Test*., **24**, 712 (2005).
[115] T. Konkhlang, K. Tashiro, M. Kotaki, S. Chirachanchai, *J. Am. Chem. Soc*., **130**, 15460 (2008).
[116] J. N. Coleman, U. Khan, Y. K. Gun'ko, *Adv. Mater*., **18**, 689 (2006).
[117] L. S. Schadler, S. C. Giannaris, P. M. Ajayan, *Appl. Phys. Lett*., **73**, 3842 (1998).
[118] M. M. Larijani, E. J. Khamse, Z. Asadollahi, M. Asadi, *Bull. Mater. Sci*., **32**, 305 (2012).
[119] Q. Wang, J. Dai, W. Li, Z. Wei, J. Jiang, *Compos. Sci. Technol*., **68**, 1644 (2008).
[120] X. L. Xie, Y.W. Mai, X.P. Zhou, *Mater. Sci. Eng*., **49**, 89 (2005).
[121] M. A. Hassan, *Al-Qadisiya J. Eng. Sci*., **5**, 341 (2012).
[122] S. Bal, S.S. Samal, *Bull. Mater. Sci*., **30**, 379 (2007).
[123] L. R. Xu, S. Sengupta, *J. Nanosci. Nanotechnol*., **5**, 620 (2005).
[124] M. Pandurangappa, G.K. Raghu, in "Carbon Nanotubes Applications on Electron Devices", edited by J. M. Marulanda, InTech, 2011, pp. 499-526.
[125] H. T. Ham, C. M. Koo, S. O. Kim, Y. S. Choi, I. J. Chung, *Macromol. Res*., **12**, 384 (2004).
[126] F. A. Abuilaiwi, T. Laoui, M. Al-Harthi, M. A. Atieh, *Arab. J. Sci. Eng*., **35**, 37 (2010).
[127] R. Andrews, M. C. Weisenberger, *Curr. Opin. Solid St. M*., **8**, 31 (2004).
[128] S. Y. Chew, T. C. Hufnagel, C. T. Lim, K. W. Leong, *Nanotechnology*, **17**, 3880 (2006).
[129] S. Y. Gu, Q. L. Wu, J. Ren, G. J. Vancso, *Macromol. Rapid. Comm*., **26**, 716 (2005).
[130] E. P. S. Tan, C. N. Goh, C. H. Sow, C. T. Lim, *Appl. Phys. Lett*., **86**, 073115 (2005).
[131] L. Yang, C. F. C. Fitié, K. O. van der Werf, M. L. Bennink, P. J. Dijkstra *et al*., *Biomaterials*, **29**, 955 (2008).
[132] D. Almecija, D. Blond, J. E. Sader, J. N. Coleman, J. J. Boland, *Carbon*, **47**, 2253 (2009).
[133] E. P. S. Tan, C. T. Lim, *Compos. Sci. Technol*., **66**, 1102 (2006).
[134] M. Gandhi, H. Yang, L. Shor, F. Ko, *Polymer*, **50**, 1918 (2009).
[135] Z. M. Huang, Y. Z. Zhang, M. Kotaki, S. Ramakrishna, *Compos. Sci. Technol*., **63**, 2223 (2003).
[136] Q. P. Pham, U. Shamra, A. G. Mikos, *Tissue Eng*., **12**, 1197 (2006).
[137] A. L. Andrady, "Science and Technology of Polymer Nanofibers", Wiley, Canada, 2008.
[138] J. H. He, Y. Liu, L. F. Mo, Y. Q. Wan, L. Xu, "Electrospun Nanofibers and Their Applications", *i*Smithers, UK, 2008.
[139] S. Ramakrishna, K. Fujihara, W. E. Teo, T. C. Lim, Z. Ma, "An Introduction to Electrospinning and Nanofibers", World Scientific Publishing, Singapore, 2005.
[140] P. J. Brown, K. Stevens, "Nanofibers and Nanotechnology in Textiles", Woodhead, England, 2007.
[141] H. L. Schreuder-Gibson, P. Gibson, K. Senecal, M. Sennett, J. Walker *et al*., *J. Adv. Mater*., **34**, 44 (2002).
[142] J. Fang, H. T. Niu, T. Lin, W. G. Wang, *Chinese Sci. Bull*., **53**, 2265 (2008).
[143] D. K. Kim, S. H. Park, B. C. Kim, B. D. Chin, S. M. Jo *et al*., *Macromol. Res*., **13**, 521 (2005).

[144] Z. Ma, M. Kotaki, T. Yong, W. He, S. Ramakrishna, *Biomaterials*, **26**, 2527 (2005).
[145] B. O. Lee, W. J. Woo, M. S. Kim, *Macromol. Mater. Eng.*, **286**, 114 (2001).
[146] Z. G. Wang, Z. K. Xu, L. S. Wan, J. Wu, *Macromol. Rapid. Comm.*, **27**, 516 (2006).
[147] M. A. Shokrgozar, F. Mottaghitalab, V. Mottaghitalab, M. Farokhi, *J. Biomed. Nanotechnol.*, **7**, 276 (2011).
[148] J. S. Im, J. G. Kim, S. H. Lee, Y. S. Lee, *Colloid. Surface A*, **364**, 151 (2010).
[149] Q. Jiang, G. Fu, D. Xie, S. Jiang, Z. Chen *et al.*, *Proced. Eng.*, **27**, 72 (2012).
[150] Y. Wanna, S. Pratontep, A. Wisitsoraat, A. Tuantranont, *Procs. 5th IEEE Conference on Sensors*, 2006, pp. 342-345.
[151] S. A. Abdullah, L. Frormann, in "Nanofibers: Fabrication, Performance, and Applications", edited by W. N. Chang, Nova Science Publishers, New York, 2009, pp. 395-410.
[152] M. M. Shokrieh, R. Rafiee, *Mater. Design*, **31**, 790 (2010).
[153] K. I. Tserpes, P. Papanikos, *Compos. Part. B*, **36**, 468 (2005).
[154] A. G. Arani, R. Rahmani, A. Arefmanesh, *Physica E.*, **40**, 2390 (2008).
[155] R. S. Ruoff, D. Qian, W. K. Liu, *C. R. Physique*, **4**, 993 (2003).
[156] X. Guo, A. Y. T. Leung, X. Q. He, H. Jiang, Y. Huang, *Compos. Part B.*, **39**, 202 (2008).
[157] J. R. Xiao, B. A. Gama, J. W. Gillespie Jr, *Int. J. Solids Struct.*, **42**, 3075 (2005).
[158] R. Ansari, B. Motevalli, *Commun. Nonlinear Sci. Numer. Simulat.*, **14**, 4246 (2009).
[159] C. Li, T. W. Chou, *Mech. Mater.*, **36**, 1047 (2004).
[160] T. Natsuki, M. Endo, *Carbon*, **42**, 2147 (2004).
[161] R. Ansari, F. Sadeghi, B. Motevalli, *Commun. Nonlinear Sci. Numer. Simulat.*, **18**, 769 (2013).
[162] F. Alisafaei, R. Ansari, *Comp. Mater. Sci.*, **50**, 1406 (2011).
[163] T. Natsuki, Q. Q. Ni, M. Endo, *Appl. Phys. A.*, **90**, 441 (2008).
[164] U. A. Joshi, S. C. Sharma, S. P. Harsha, *Proc. IMechE., Part N: J. Nanoeng. Nanosys.*, **225**, 23 (2011).
[165] G. M. Odegard, T. S. Gates, L. M. Nicholson, K. E. Wise, *Compos. Sci. Technol.*, **62**, 1869 (2002).
[166] C. Li, T. W. Chou, *Int. J. Solids Struct.*, **40**, 2487 (2003).
[167] Y. I. Prylutskyy, S. S. Durov, O. V. Ogloblya, E. V. Buzaneva, P. Scharff, *Comp. Mater. Sci.*, **17**, 352 (2000).
[168] B. I. Yakobson, C. J. Brabec, J. Bernholc, *Phys. Rev. Lett.*, **76**, 2511 (1996).
[169] Y. Jin, F. G. Yuan, *Compos. Sci. Technol.*, **63**, 1507 (2003).
[170] G. V. Lier, C. V. Alsenoy, V. V. Doren, P. Geerlings, *Chem. Phys. Lett.*, **326**, 181 (2000)
[171] K. N. Kudin, G. E. Scuseria, B. I. Yakobson, *Phys. Rev. B.*, **64**, 235406 (2001).
[172] E. Hernandez, C. Goze, P. Bernier, A. Rubio, *Phys. Rev. Lett.*, **80**, 4502 (1998).
[173] Z. Xin, Z. Jianjun, O. Y. Zhong-can, *Phys. Rev. B.*, **62**, 13692 (2000).
[174] E. Hernandez, C. Goze, P. Bernier, A. Rubio, *Appl. Phys. A.*, **68**, 287 (1999).
[175] T. Chang, H. Gao, *J. Mech. Phys. Solids*, **51**, 1059 (2003).
[176] B. I. Yakobson, C. J. Brabec, J. Bernholc, *Phys. Rev. Lett.*, **76**, 2511 (1996).
[177] P. Zhang, Y. Huang, P. H. Geubelle, P. A. Klein, K. C. Hwang, *Int. J. Solids Struct.*, **39**, 3893 (2002).
[178] Z. Tu, Z. Ou-Yang, *Phys. Rev. B.*, **65**, 233407 (2002).
[179] C. Y. Li, T. W. Chou, *Compos. Sci. Technol.*, **63**, 1517 (2003).
[180] T. Vodenitcharova, L. C. Zhang, *Phys. Rev. B.*, **68**, 165401 (2003).
[181] Q. Wang, *Int. J. Solids Struct.*, **41**, 5451 (2004).
[182] A. Selmi, C. Friebel, I. Doghri, H. Hassis, *Compos. Sci. Technol.*, **67**, 2071 (2007).
[183] A. Pantano, D. M. Parks, M.C. Boyce, *J. Mech. Phys. Solids*, **52**, 789 (2004).
[184] X. Sun, W. Zhao, *Mater. Sci. Eng. A*, **390**, 366 (2005).
[185] A. L. Kalamkarov, A. V. Georgiades, S. K. Rokkam, V. P. Veedu, M. N. Ghasemi-Nejhad, *Int. J. Solids Struct.*, **43**, 6832 (2006).
[186] P. Papanikos, D. D. Nikolopoulos, K. I. Tserpes, *Comput. Mater. Sci.*, **43**, 345 (2008).
[187] M. M. Treacy, T. W. Ebbesen, J. M. Gibson, *Nature*, **38**, 678 (1996).
[188] O. Lourie, D. M. Cox, H. D. Wagner, *Phys. Rev. Lett.*, **81**, 1638 (1998).
[189] J. Z. Liu, Q. S. Zheng, Q. Jiang, *Phys. Rev. Lett.*, **86**, 4843 (2001).
[190] M. F. Yu, O. Lourie, M. J. Dyer, K. Moloni, T. F. Kelly *et al.*, *Science*, **287**, 637 (2000)
[191] T. W. Tombler, C. Zhou, J. Kong, H. Dai, L. Liu *et al.*, *Nature*, **405**, 769 (2000).
[192] A. Krishnan, E. Dujardin, T. W. Ebbesen, P. N. Yianilos, M. M. J. Treacy, *Phys. Rev. B.*, **58**, 14013 (1998).
[193] M. M. Shokrieh, R. Rafiee, *Mech. Res. Commun.*, **37**, 235 (2010).
[194] K. I. Tserpes, P. Papanikos, G. Labeas, Sp. G. Pantelakis, *Theor. Appl. Fract. Mec.*, **49**, 51 (2008).
[195] R. G. Villoria, A. Miravete, *Acta Mater.*, **55**, 3025 (2007).
[196] S. J. V. Frankland, V. M. Harik, G. M. Odegard, D. W. Brenner, T. S. Gates, *Compos. Sci. Technol.*, **63**, 1655 (2003).
[197] G. M. Odegard, T. S. Gates, K. E. Wise, C. Parka, E. J. Siochi, *Compos. Sci. Technol.*, **63**, 1671 (2003).

[198] K. P. A. Saffar, N. J. Pour, A. R. Najafi, G. Rouhi, A. R. Arshi *et al*., *World Acad. Sci. Eng. Tech*., **47**, 219 (2008).
[199] A. Haque, A. Ramasetty, *Compos. Struct*., **71**, 68 (2005).
[200] K. Q. Xiao, L. C. Zhang, *J. Mater. Sci*., **39**, 4481 (2004).
[201] A. E. Eken, E. J. Tozzi, D. J. Klingenberg, W. Bauhofer, *Polymer*, **53**, 4493 (2012).
[202] S. K. Georgantzinos, G. I. Giannopoulos, N. K. Anifantis, *Theor. Appl. Fract. Mec*., **52**, 158 (2009).
[203] H. Wang, F. Meng, X. Wang, *J. Reinf. Plast. Comp*., **29**, 2262 (2010).
[204] V. U. Unnikrishnan, G. U. Unnikrishnan, J. N. Reddy, *Compos. Struct*., **93**, 1008 (2011)
[205] T. Takeda, Y. Shindo, F. Narita, Y. Mito, *Mater. Trans*., **50**, 436 (2009).